

# Optical Axial Chirality Enhancement and Transfer within Aromatic Micelles upon (Co-)encapsulation

Tomohiro Yasuda, Yoshihisa Hashimoto, Yuya Tanaka,\* Daiki Tauchi, Masashi Hasegawa, Yusuke Kurita, Hidetoshi Kawai, Yoshitaka Tsuchido,\* and Michito Yoshizawa\*



Cite This: *JACS Au* 2025, 5, 586–592



Read Online

ACCESS |

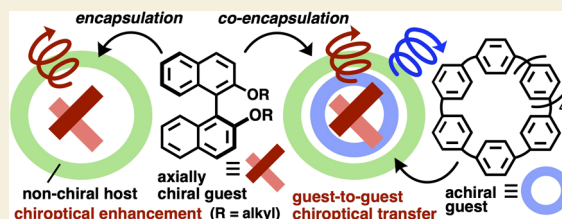
Metrics & More

Article Recommendations

Supporting Information

**ABSTRACT:** Axial chirality is the key physiochemical element, yet its chiroptical utilities have been largely limited to covalent synthesis and infinitely assembled systems so far. Here we report a new application of axially chiral binaphthyls for efficient, optical chirality enhancement and transfer upon noncovalent encapsulation by achiral aromatic micelles in water. The CD activities of dialkoxy binaphthyls are significantly enhanced (up to 7-fold) upon encapsulation by an anthracene-based aromatic micelle. Large emission enhancement ( $\sim 4$ -fold) and efficient guest-to-guest, optical chirality transfer are achieved through coencapsulation of the binaphthyls with achiral cycloparaphenylenes, in a guest-within-guest fashion, by the micelle. The observed unusual properties are derived from the tight inclusion of the chiral guests into the macrocyclic guests, efficiently generated only in the aromatic cavity. Moderate CPL can be observed from the coencapsulated macrocycles within the ternary composites. Furthermore, more than  $\sim 4$ -fold enhanced guest-to-guest chiroptical transfer is demonstrated with a functionalized cycloparaphenylene through the present coencapsulation strategy.

**KEYWORDS:** axial chirality transfer, binaphthyl compounds, coencapsulation, cycloparaphenylene, aromatic micelle



Axial chirality, based on restricted rotation around a single bond, is typically found in biaryl compounds.<sup>1</sup> Unlike central and planar chiralities, the chiral properties largely depend on the dihedral angle between the aromatic panels. Among them, binaphthyl is one of the most useful, axially chiral components, e.g., for applications in enantioselective sensors, chiroptical materials, and asymmetric catalysis,<sup>2</sup> due to the high configurational stability, asymmetrical bulkiness, and synthetical accessibility. To further enhance and expand the characteristic chiroptical functions, the development of rational chirality transfer systems from axially chiral components to nonchiral dyes is much in demand at the molecular level. The majority of the studies have been performed with covalent linkages (Figure 1a), e.g., employing perylene bisimide and boron-dipyrromethene dyes,<sup>3</sup> as well as infinite molecular assemblies.<sup>4</sup> Whereas efficient, optical chirality transfer can be found by these methods, laborious syntheses or huge assemblies are usually required. Finite host–guest complexation is an alternative method, using chiral hosts and achiral dye guests.<sup>5</sup> Various cage-shaped hosts have been prepared so far, e.g., from metal hinges and organic ligands embedding axially chiral units (Figure 1b). However, efficient host-to-guest chirality transfer was seldom accomplished in the cavity, owing to weak or no host–guest interactions.<sup>6</sup> To advance the host–guest methodology, here we propose a new coencapsulation strategy by combining axially chiral compounds and achiral dyes with a non-chiral host (Figure 1c).

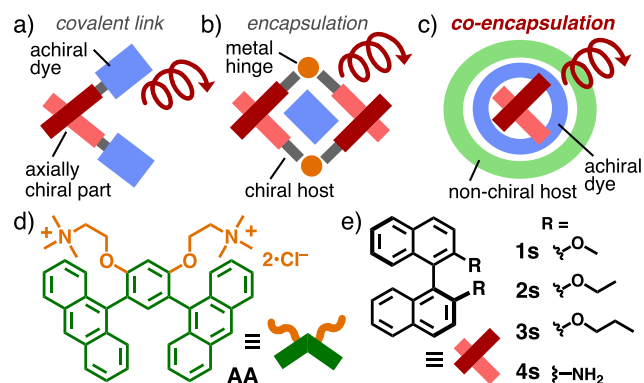


**Figure 1.** Schematic representation of optical axial chirality transfer systems: a) a covalent compound and noncovalent host–guest composites using b) a chiral host and c) a nonchiral host (this work). d) Bent aromatic amphiphile AA and e) (S)-binaphthyl derivatives 1–4s.

Received: December 17, 2024

Revised: January 9, 2025

Accepted: January 27, 2025

Published: February 3, 2025



We herein report (i) the circular dichroism (CD) enhancement of binaphthyl derivatives (up to 6.9-fold) upon encapsulation by achiral aromatic micelles in water, (ii) the emission enhancement of cycloparaphenylene dyes in the micelle (up to 4.3-fold;  $\Phi_F = 86\%$ ) upon coencapsulation with binaphthyls, (iii) efficient guest-to-guest, optical chirality transfer to the achiral macrocycles ( $|g_{abs}| = \text{up to } 2.4 \times 10^{-4}$ ), and (iv) the unusual observation of circularly polarized luminescence (CPL;  $|g_{lum}| = \text{up to } 2.5 \times 10^{-4}$ ) from the coencapsulated, achiral guests. (v) The same coencapsulation protocol also enables multifunctionalized cycloparaphenylene to be chiroptically active to a large extent (i.e.,  $|g_{abs}| = 1.4 \times 10^{-3}$ ,  $|g_{lum}| = 9.5 \times 10^{-4}$ ). The present new host-guest strategy is expected to deepen and widen axial chirality-based optical chemistry.

Efficient coencapsulation of two kinds of molecules has been widely studied using both covalent/noncovalent tubular, cage-shaped, and capsular compounds.<sup>7,8</sup> Although various molecules in the range of small to large sizes could be simultaneously encapsulated by these hosts, the successful coencapsulation of axially chiral compounds with macrocyclic dyes has yet to be reported. Aromatic micelle ( $(AA)_n$ ) is an aqueous achiral capsule,<sup>9</sup> composed of bent aromatic amphiphiles **AA** (Figure 1d), featuring two anthracene panels and two ammonium groups. The discrete, adaptable polyaromatic cavity of  $(AA)_n$  can accommodate various achiral aromatic molecules (e.g., organic dyes and metal-complexes) in water, through efficient hydrophilic effect as well as  $\pi$ - $\pi$  and CH- $\pi$  interactions.<sup>10</sup> To unveil the host ability toward axially chiral compounds, in this report, we for the first time employ (S)/(R)-binaphthyl derivatives **1-4**, bearing two methoxy, ethoxy, propoxy, and amino groups, respectively (Figure 1e). [9]Cycloparaphenylene<sup>11</sup> and its multimethoxy derivative<sup>12</sup> are selected as coencapsulated dyes, with a rigid and highly symmetrical, macrocyclic framework (1.2 nm in diameter) and high/moderate emission properties, for unusual guest-to-guest, optical chirality transfer in the aromatic cavity.<sup>13,14</sup>

Axially chiral compound **1s** ((S)-isomer, R = OCH<sub>3</sub>) was efficiently encapsulated by aromatic micelle  $(AA)_n$ , superior to other micelles tested herein, in water through a grinding protocol (Figure 2a). A mixture of **AA** (1.0  $\mu\text{mol}$ ) and water-insoluble **1s** (2.0  $\mu\text{mol}$ ) was ground using a mortar and pestle for 1 min. Subsequently, water (1.0 mL) was added to the solid, and the resultant suspension was centrifuged (16000g, 10 min) and filtered (pore size: 200 nm) to yield a clear colorless solution containing host-guest composite  $(AA)_n \cdot (1s)_m$  without free **1s**.<sup>15,16</sup> The manual grinding is essential to facilitate **AA-1s** interactions prior to adding water (Figure S17). The UV-visible spectrum of the aqueous solution showed broad absorption bands at 280–350 nm, attributed to bound  $(1s)_m$ , along with the anthracene-based vibronic bands (320–420 nm) of  $(AA)_n$  (Figure 2b). The product structure, a spherical  $(AA)_{27} \cdot (1s)_{18}$  assembly on average, was revealed by DLS, NMR-based host-guest ratio, and molecular modeling analyses. The DLS chart displayed a single peak at 4.0 nm (Figure 2c), as an average core diameter of the product, in water, unlike that of empty  $(AA)_n$  ( $d_{av.} = 1.5$  nm). The <sup>1</sup>H NMR-based integrals of the isolated product (via lyophilization) in CD<sub>3</sub>CN indicated its average **AA:1s** ratio being 3:2 (Figure S7b). The molecular modeling studies based on the DLS and NMR data suggested the formation of a large spherical particle, composed of an 18-**1s** core and a 27-**AA** shell, with a calculated core diameter of 4.0 nm (Figure 2d).

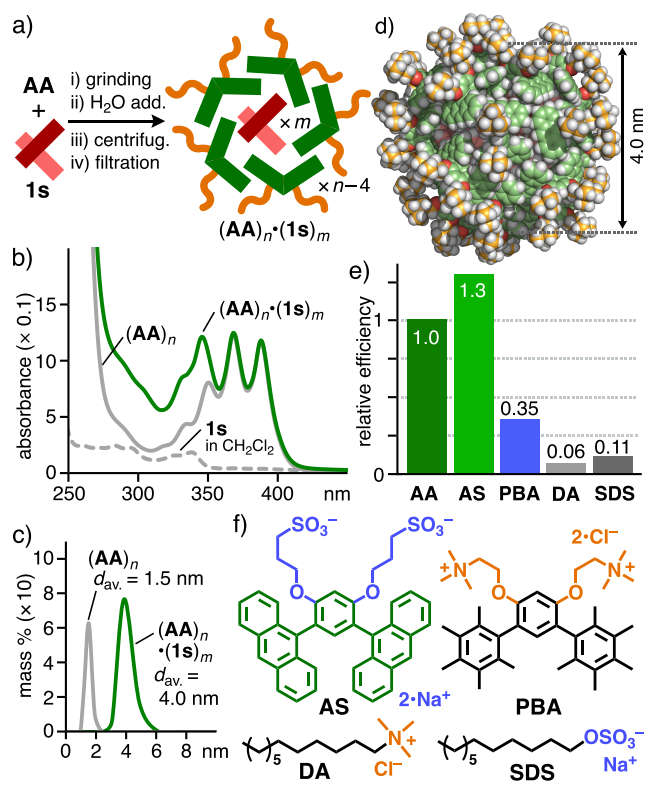


**Figure 2.** a) Formation of  $(AA)_n \cdot (1s)_m$  in water through a grinding protocol. b) UV-visible spectra (H<sub>2</sub>O, r.t., 1.0 mM based on **AA**) of  $(AA)_n \cdot (1s)_m$ ,  $(AA)_n$ , and **1s** (0.2 mM). c) DLS charts (H<sub>2</sub>O, r.t., 1.0 mM based on **AA**) of  $(AA)_n \cdot (1s)_m$  and  $(AA)_n$ . d) Optimized structure of  $(AA)_{27} \cdot (1s)_{18}$  (MM calculation). e) Relative uptake efficiency of micelles from various amphiphiles toward **1s** in water. f) Aromatic and alkyl amphiphiles studied herein.

Within the polyaromatic shell, the presence of multiple CH- $\pi$  and  $\pi$ - $\pi$  interactions in aggregated  $(1s)_m$  was also supported by the structure.<sup>15,17</sup> Typical alkyl-based micelles such as  $(DA)_n$  and  $(SDS)_n$ , in contrast, showed inefficient binding ability toward **1s** by the same protocol ( $\sim 0.1$ -fold as compared with  $(AA)_n$ ; Figure 2e,f), owing to the lack of host-guest  $\pi$ - $\pi$  interactions. Other aromatic micelles (**AS**)<sub>n</sub> featuring hydrophilic sulfonate groups and (**PBA**)<sub>n</sub> featuring hydrophobic pentamethylbenzene panels encapsulated **1s** with high and moderate efficiency relative to that of  $(AA)_n$ , respectively (Figure 2e).

The chiroptical properties (e.g., CD signal intensity and sign) of **1s** were largely altered upon encapsulation by aromatic micelles at room temperature. The CD spectrum of **1s** in CH<sub>2</sub>Cl<sub>2</sub> exhibited two negative Cotton effects at 280 and 320 nm. In contrast, that of host-guest composite  $(AA)_n \cdot (1s)_m$  in H<sub>2</sub>O showed two intense positive Cotton effects at 300 and 340 nm ( $\theta_{max} = 55$  mdeg) as well as an intense negative one at 280 nm, derived from bound  $(1s)_m$  (Figure 3a). The negative to positive inversion of the **1s**-based CD bands was thus induced through encapsulation.<sup>18</sup> Weak negative Cotton effects were also detected between 350 and 420 nm ( $\theta_{min} = -2.1$  mdeg), which is in the range of the anthracene-based absorption bands of  $(AA)_n$  (Figure 2b), suggesting optical chirality transfer from guest  $(1s)_m$  to host  $(AA)_n$ . To clarify the chirality enhancement of **1s** upon encapsulation, the CD spectrum of  $(AA)_n \cdot (1s)_m$  in CH<sub>3</sub>CN, where the host-guest composite is fully disassembled into  $n$ -**AA** and  $m$ -**1s**, was

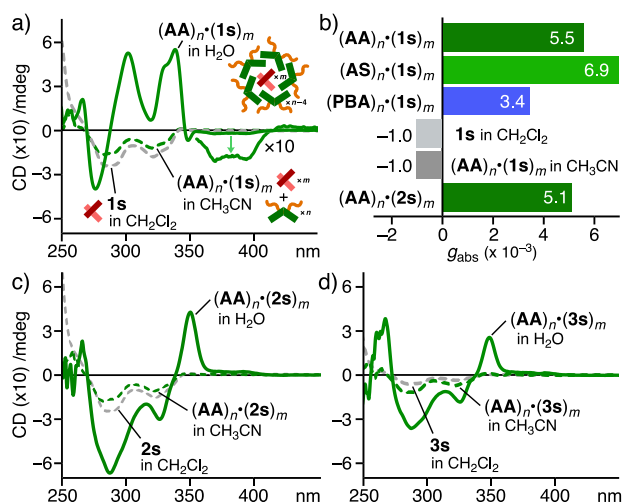


**Figure 3.** a) CD spectra (r.t., 1.0 mM based on AA) of  $(AA)_n \cdot (1s)_m$ , **1s** (0.4 mM), and disassembled  $(AA)_n \cdot (1s)_m$ . b) Maximum  $g_{\text{abs}}$  values ( $H_2O$ , r.t., 1.0 mM based on amphiphiles) of  $(AA)$  or  $AS$  or  $PBA$   $\cdot (1s)$  or  $2s$   $\cdot 1s$ , and disassembled  $(AA)_n \cdot (1s)_m$ . CD spectra (rt, 1.0 mM based on AA) of c)  $(AA)_n \cdot (2s)_m$ , **2s** (0.5 mM), and disassembled  $(AA)_n \cdot (2s)_m$  and d)  $(AA)_n \cdot (3s)_m$ , **3s** (0.3 mM), and disassembled  $(AA)_n \cdot (3s)_m$ .

observed after lyophilization of the aqueous  $(AA)_n \cdot (1s)_m$  solution. The spectrum shape was comparable to that of free **1s** in  $CH_2Cl_2$ , and no CD band was detected at 350–420 nm (Figure 3a). Notably, the absolute CD intensity of  $(AA)_n \cdot (1s)_m$  in  $H_2O$  (absolute absorption dissymmetry factor ( $|g_{\text{abs}}|$ ) =  $5.5 \times 10^{-3}$ ,  $\lambda = 301$  nm) was enhanced by 5.5-fold, as compared to those of **1s** in  $CH_2Cl_2$  and disassembled  $(AA)_n \cdot (1s)_m$  in  $CH_3CN$  ( $|g_{\text{abs}}| = 1.0 \times 10^{-3}$ ,  $\theta_{\text{min}} = -17$  mdeg,  $\lambda = 282$  nm; Figure 3b).<sup>19</sup> Further CD enhancement of **1s** (6.9-fold) was observed upon encapsulation by sulfonate-based aromatic micelle ( $AS$ )<sub>n</sub> in  $H_2O$  (Figure 2f, 3b, and S12). On the other hand, host–guest composites ( $PBA$  or  $DA$  or  $SDS$ )<sub>n</sub>  $\cdot (1s)_m$  showed weaker CD bands ( $\theta_{\text{max}} = 3$ –18 mdeg; Figure S12) with moderate  $|g_{\text{abs}}|$  values ( $3.4$ – $3.9 \times 10^{-3}$ ) under the same conditions. The observed CD enhancement and inversion of **1s** within  $(AA)_n$  stem from the tight aggregation of  $m$ -**1s**,<sup>20</sup> accompanying the alteration of the dihedral angle ( $\varphi$ ) of **1s**, in the polyaromatic cavity.<sup>21,22</sup>

Dialkoxy substituents on the binaphthyl largely altered the chiroptical properties of the resultant host–guest composites in water. The CD spectrum of  $(AA)_n \cdot (2s)_m$  prepared from AA and ethoxy derivative **2s** in the same manner as  $(AA)_n \cdot (1s)_m$ <sup>15</sup> exhibited a strong negative and positive Cotton effect at 280 and 350 nm ( $\theta_{\text{min}} = -67$  mdeg), respectively (Figure 3c). The maximum intensity of the absolute CD bands ( $|g_{\text{abs}}| = 5.1 \times 10^{-3}$ ,  $\lambda = 286$  nm) was 4.0-fold higher than that of dissociated  $(AA)_n \cdot (2s)_m$  in  $CH_3CN$  ( $\lambda = 282$  nm) and comparable to that of  $(AA)_n \cdot (1s)_m$  in water (Figure 3b). The CD spectrum of  $(AA)_n \cdot (3s)_m$  ( $R = OCH_2CH_2CH_3$ ) was similar to that of  $(AA)_n \cdot (2s)_m$  with weaker intensity ( $|g_{\text{abs}}| = 4.1 \times 10^{-3}$ ,  $\lambda = 286$  nm, Figure 3d). Within the aromatic micelle, accordingly, the aggregation-induced chiroptical properties of binaphthyls could be tuned (i.e.,  $\sim 3$ – $6$  times) by a slight change in the alkoxy substituents.

Next, (1) efficient coencapsulation of axially chiral compounds **2s** ( $R = OCH_2CH_3$ ) with achiral macrocycle dyes, (2) emission enhancement of the coencapsulated dyes, and (3) guest-to-guest optical chirality transfer were

demonstrated within aromatic micelle  $(AA)_n$ . As such an achiral dye, hydrophobic [9]cycloparaphenylene (**CP**,  $X = H$ ; Figure 4b) was employed to facilitate tight guest–guest

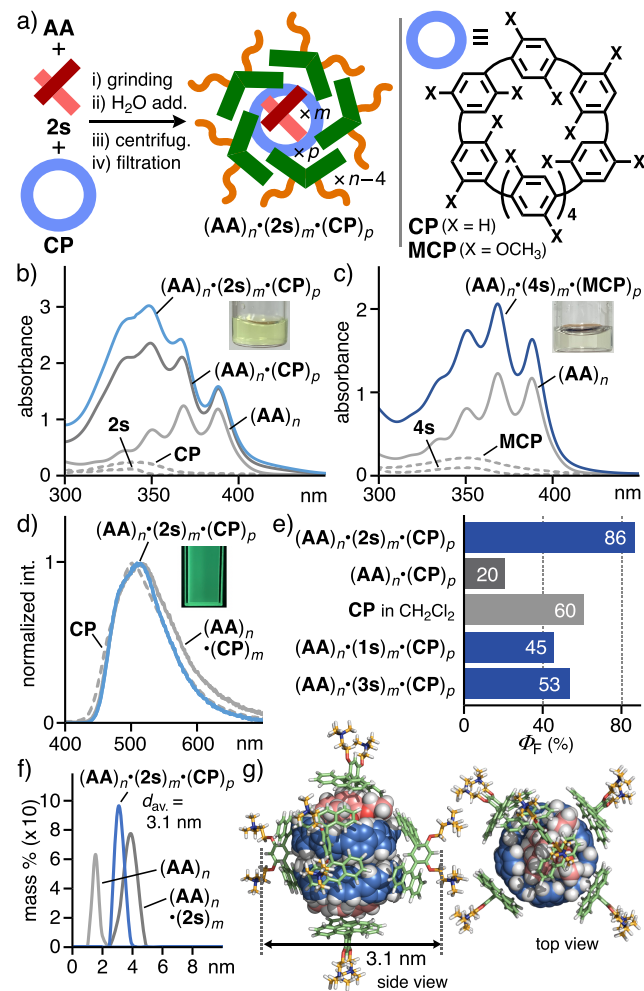


**Figure 4.** a) Formation of  $(AA)_n \cdot (2s)_m \cdot (CP)_p$  in water. UV–visible spectra ( $H_2O$ , r.t., 1.0 mM based on AA) of b)  $(AA)_n \cdot (2s)_m \cdot (CP)_p$ ,  $(AA)_n \cdot (CP)_p$ ,  $(AA)_n$ , and **CP** (0.01 mM) and **2s** (0.1 mM) in  $CH_2Cl_2$ , and c)  $(AA)_n \cdot (4s)_m \cdot (MCP)_p$ ,  $(AA)_n$ , and **MCP** (0.01 mM) and **4s** (0.1 mM) in  $CH_2Cl_2$ . d) Fluorescence spectra ( $H_2O$ , r.t.,  $\lambda_{\text{ex}} = 300$  nm, 1.0 mM based on AA) of  $(AA)_n \cdot (2s)_m \cdot (CP)_p$ ,  $(AA)_n \cdot (CP)_p$ , and **CP** (0.01 mM) in  $CHCl_3$ . e) Emission quantum yields ( $H_2O$ , r.t.,  $\lambda_{\text{ex}} = 325, 340, 305$  nm) of host–guest composites, and **CP** (0.1 mM). f) DLS charts ( $H_2O$ , r.t., 1.0 mM based on AA) of  $(AA)_n \cdot (2s)_m \cdot (CP)_p$ ,  $(AA)_n \cdot (2s)_m$ , and  $(AA)_n$ . g) Optimized structure of  $(AA)_6 \cdot (2s)_2 \cdot (CP)_2$  (MM calculation).

interactions with **2s** in the macrocyclic cavity. The absorption and emission wavelengths of **CP** are obviously different from those of  $(AA)_n$ . Coencapsulation of **2s** and **CP** by  $(AA)_n$  was carried out through a three-component grinding protocol. A mixture of solids AA and **2s** (1.0  $\mu\text{mol}$  each), and **CP** (0.5  $\mu\text{mol}$ ) was manually ground for 1 min. After the addition of water (1.0 mL) and complete removal of the suspended solid of free **2s** and **CP**, ternary host–guest composite  $(AA)_n \cdot (2s)_m \cdot (CP)_p$  was obtained as a yellow aqueous solution (Figure 4a).<sup>15</sup> The composition and structure of  $(AA)_n \cdot (2s)_m \cdot (CP)_p$  were carefully revealed by a combination of UV–visible, DLS, NMR, and molecular modeling analyses. The UV–visible spectrum of the resultant solution showed broad bands at

300–370 nm, derived from encapsulated  $(2s)_m$  and  $(CP)_p$ , besides bands at 320–420 nm from  $(AA)_n$  (Figure 4b). The DLS analysis indicated the core diameter of the product being 3.1 nm on average (Figure 4f), unlike those of  $(AA)_n$  and  $(AA)_n \cdot (2s)_m$ . The average AA:2s:CP ratio of the product was estimated to be 3:1:1 by the  $^1H$  NMR study (Figure S19b).<sup>15</sup> These results suggested that the obtained composite provides a hydrophobic core, comprising two molecules of CP accommodating two molecules of 2s, surrounded by a polyaromatic shell, formed from six molecules of AA, through molecular modeling studies (Figure 4g).<sup>23</sup>

It is noteworthy that the ternary host–guest composite  $(AA)_n \cdot (2s)_m \cdot (CP)_p$  emitted strong green fluorescence derived from bound CP in water. In the fluorescence spectrum, intense emission bands were observed at  $\lambda_{max} = 507$  nm with a high quantum yield ( $\Phi_F = 86\%$ ; Figure 4d). The yield is 4.3-fold higher than that of  $(AA)_n \cdot (CP)_p$  in water ( $\Phi_F = 20\%$ ) and 1.4-fold higher than that of free CP in  $CHCl_3$  ( $\Phi_F = 60\%$ ; Figure 4e). Ternary host–guest composites  $(AA)_n \cdot (1s)_m \cdot (CP)_p$  and  $(AA)_n \cdot (3s)_m \cdot (CP)_p$  were also prepared using AA, CP, and 1/3s ( $R = OCH_3/OCH_2CH_2CH_3$ ; Figure S29–S33). The resultant composites showed green emission with  $\Phi_F = 45\%$  ( $\lambda_{max} = 519$  nm) and 53% ( $\lambda_{max} = 512$  nm), respectively (Figure 4e). On the other hand, relatively weak emission ( $\Phi_F = 10\%$ ) was detected from sulfonate-based composite  $(AS)_n \cdot (2s)_m \cdot (CP)_p$  under the same conditions (Figure S33a).<sup>15,16d</sup> The observed emission enhancement within  $(AA)_n$  is most probably caused by CH- $\pi$ -based guest–guest interactions between 2s and CP (Figure 4g), which suppresses its thermal deactivation through dynamic motion upon excitation.<sup>24</sup> Notably, the quantum yield of  $(AA)_n \cdot (2s)_m \cdot (CP)_p$  ( $\Phi_F = 86\%$ ) represents the quite high value, observed among CP reported previously,<sup>25</sup> even under ambient aqueous conditions.

Optical chirality transfer from guests 2s to CP within the discrete aromatic micelle was clearly confirmed by CD and CPL analyses. In the CD spectrum of  $(AA)_n \cdot (2s)_m \cdot (CP)_p$  in water, a new positive Cotton effect was observed at 350–400 nm ( $|g_{abs}| = 1.4 \times 10^{-4}$ ,  $\lambda = 368$  nm; Figure 5a,e), which coincides with the absorption band of  $(CP)_p$  within  $(AA)_n$  (Figure 4b), combined with the 2s-based positive Cotton effect at 330–360 nm. The mirror symmetric CD spectrum ( $|g_{abs}| = 1.2 \times 10^{-4}$ ) was displayed from its enantiomer  $(AA)_n \cdot (2r)_m \cdot (CP)_p$ . The observed CP-based bands stem from efficient chirality transfer from 2s/r to CP through simple coencapsulation by micelle  $(AA)_n$ .<sup>26</sup> In contrast, the CP-based CD bands hardly appeared in the spectra of  $(DA)_n \cdot (2s)_m \cdot (CP)_p$  and  $(AS)_n \cdot (2s)_m \cdot (CP)_p$  even under the same conditions (Figure 5e and S26b,27b). These results also clarified the exact formation of the guest-within-guest ternary structure (Figure 4g) as a major product. The CPL spectra of  $(AA)_n \cdot (2s)_m \cdot (CP)_p$  and  $(AA)_n \cdot (2r)_m \cdot (CP)_p$  showed roughly symmetric mirror bands in the range between 450 and 660 nm (Figure 5b), which corresponds to the emission band of CP (Figure 4d). The absolute emission asymmetry factors ( $|g_{lum}|$ ) of the host–guest composites were estimated to be  $2.0 \times 10^{-4}$  ( $\lambda = 510$  nm; Figure 5f). The observed CPL, derived from guest-to-guest optical chirality transfer in host compounds, is quite uncommon in various host–guest CPL systems reported previously.<sup>27</sup>

To deepen the understanding of the observed chirality transfer, chiroptical studies of various host–guest composites were examined under the same aqueous conditions. The CP-based CD bands of  $(AA)_n \cdot (1s$  or  $2s$  or  $3s)_m \cdot (CP)_p$  at 360 nm

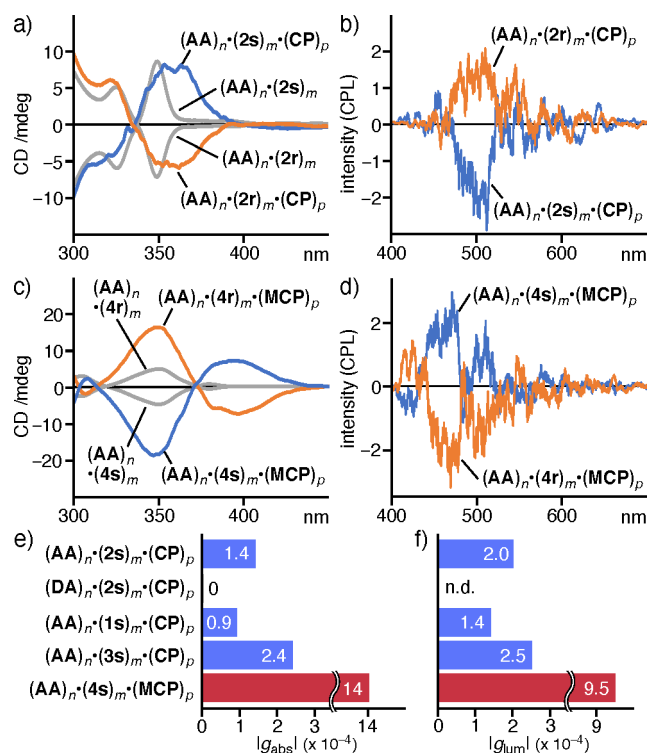


**Figure 5.** a) CD spectra ( $H_2O$ , r.t., 1.0 mM based on AA) of  $(AA)_n \cdot (2s$  or  $2r)_m \cdot (CP)_p$  and  $(AA)_n \cdot (2s$  or  $2r)_m$  and b) their selected CPL spectra ( $\lambda_{ex} = 325$  nm). c) CD spectra ( $H_2O$ , r.t., 1.0 mM based on AA) of  $(AA)_n \cdot (4s$  or  $4r)_m \cdot (MCP)_p$  and  $(AA)_n \cdot (4s$  or  $4r)_m$  and d) their selected CPL spectra ( $\lambda_{ex} = 300$  nm). e) CP/MCP-based maximum  $|g_{abs}|$  and f)  $|g_{lum}|$  values ( $H_2O$ , r.t.,  $\lambda_{ex} = 340, 305$  nm) of various host–guest composites.

indicated that binaphthyl with longer alkoxy groups ( $R = OCH_2CH_2CH_3$ ;  $|g_{abs}| = 2.4 \times 10^{-4}$ ) is more effective in the chirality transfer than that with shorter ones ( $R = OCH_3$ ;  $|g_{abs}| = 0.9 \times 10^{-4}$ ; Figure 5e). No guest–guest interaction was found between 2s and CP without AA in solution (Figure S28).<sup>15</sup> The CD spectrum of  $(PBA)_n \cdot (2s)_m \cdot (CP)_p$  also displayed a CP-based band at  $\sim 400$  nm ( $|g_{abs}| = 0.6 \times 10^{-4}$ ; Figure S22), suggesting the importance of the polyaromatic host framework in this system. Size/shape complementarity and CH- $\pi$ -based guest–guest interactions in the cyclic guest cavity are essential for the observed chirality transfer because no dye-based CD band was detected from  $(AA)_n \cdot (2s)_m \cdot ([12]cycloparaphenylene)_p$  under the same conditions (Figure S23), owing to its large macrocyclic framework (1.7 nm in diameter). Composites  $(AA)_n \cdot (1s$  or  $3s)_m \cdot (CP)_p$  exhibited CPL bands at 450–660 nm (Figure 5e and S45,S47), with medium  $|g_{lum}|$  values in water ( $|g_{lum}| = 1.4$  and  $2.5 \times 10^{-4}$ , respectively). Furthermore, efficient guest-to-guest chiroptical transfer could be also applied to sterically hindered, multi-methoxy functionalized [9]cycloparaphenylene (MCP; Figure 4a, right) upon coencapsulation with diamino binaphthyls 4s/r without bulky substituents ( $R = NH_2$ ; Figure 1e).<sup>12b,15</sup> An intense CD band at 370–450 nm ( $|g_{abs}| = 1.4 \times 10^{-3}$ ,  $\lambda = 396$  nm) and CPL bands at 400–600 nm ( $|g_{lum}| = 9.5 \times 10^{-4}$ ,  $\lambda = 476$  nm) were notably observed in the chiroptical spectra of  $(AA)_n \cdot (4s$  or  $4r)_m \cdot (MCP)_p$  in water (Figure 5c and 5d, respectively). The large enhancement of the observed  $|g_{abs}|$  and  $|g_{lum}|$  values (i.e., 3.8 to 15.6-fold) through guest replacement from achiral dyes CP to MCP is most likely attributed to the

enhanced conformational rigidity of the macrocyclic framework (e.g., induced planar chirality) by the sterically demanding methoxy groups (Figure 5e,f).

In summary, we have succeeded in the effective enhancement and transfer of the chiroptical properties of axially chiral binaphthyls within nonchiral aromatic micelles, with dimensions of ~3–4 nm. Both phenomena were generated upon simple encapsulation with or without cycloparaphenylenes under ambient aqueous conditions. Large CD enhancement of the binaphthyl compounds was observed in the cavity. Coencapsulation of the chiral compounds with the achiral macrocycles led to the selective formation of guest-within-guest ternary composites, providing macrocycle-based, high emissivity, as well as CPL activities, via unusual “guest-to-guest” chirality transfer. Thanks to the finite, adaptable host frameworks of the aromatic micelles and high accessibility to axially chiral compounds, we believe that the present, simple coencapsulation strategy could be applied for wide-ranging nonchiral dyes and metal-complexes<sup>28</sup> to generate new chiroptical materials and chiral catalysts, respectively, without elaborate chiral functionalization on the guest frameworks.

## ■ ASSOCIATED CONTENT

### Data Availability Statement

The data underlying this study are available in the published article and its Supporting Information.

### SI Supporting Information

The Supporting Information is available free of charge at <https://pubs.acs.org/doi/10.1021/jacsau.4c01229>.

Experimental procedures; NMR, MS, IR, UV–visible, fluorescence, DLS, CD, CPL, and calculation data (PDF)

## ■ AUTHOR INFORMATION

### Corresponding Authors

**Yuya Tanaka** – Laboratory for Chemistry and Life Science, Institute of Integrated Research, Institute of Science Tokyo, Yokohama 226-8501, Japan; [orcid.org/0000-0002-0674-660X](https://orcid.org/0000-0002-0674-660X); Email: [ytanaka@res.titech.ac.jp](mailto:ytanaka@res.titech.ac.jp)

**Yoshitaka Tsuchido** – Department of Chemistry, Faculty of Science, Tokyo University of Science, Shinjuku-ku, Tokyo 162-8601, Japan; [orcid.org/0000-0001-8860-0745](https://orcid.org/0000-0001-8860-0745); Email: [tsuchido@rs.tus.ac.jp](mailto:tsuchido@rs.tus.ac.jp)

**Michito Yoshizawa** – Laboratory for Chemistry and Life Science, Institute of Integrated Research, Institute of Science Tokyo, Yokohama 226-8501, Japan; [orcid.org/0000-0002-0543-3943](https://orcid.org/0000-0002-0543-3943); Email: [yoshizawa.m.ac@m.titech.ac.jp](mailto:yoshizawa.m.ac@m.titech.ac.jp)

### Authors

**Tomohiro Yasuda** – Laboratory for Chemistry and Life Science, Institute of Integrated Research, Institute of Science Tokyo, Yokohama 226-8501, Japan

**Yoshihisa Hashimoto** – Laboratory for Chemistry and Life Science, Institute of Integrated Research, Institute of Science Tokyo, Yokohama 226-8501, Japan

**Daiki Tauchi** – Department of Chemistry, Graduate School of Science, Kitasato University, Sagami-hara, Kanagawa 252-0373, Japan

**Masashi Hasegawa** – Department of Chemistry, Graduate School of Science, Kitasato University, Sagami-hara,

Kanagawa 252-0373, Japan; [orcid.org/0000-0003-3302-6496](https://orcid.org/0000-0003-3302-6496)

**Yusuke Kurita** – Department of Chemistry, Faculty of Science, Tokyo University of Science, Shinjuku-ku, Tokyo 162-8601, Japan

**Hidetoshi Kawai** – Department of Chemistry, Faculty of Science, Tokyo University of Science, Shinjuku-ku, Tokyo 162-8601, Japan; [orcid.org/0000-0002-3367-0153](https://orcid.org/0000-0002-3367-0153)

Complete contact information is available at: <https://pubs.acs.org/doi/10.1021/jacsau.4c01229>

## Notes

The authors declare no competing financial interest.

## ■ ACKNOWLEDGMENTS

This work was supported by JSPS KAKENHI (Grant No. JP21K05211/JP22H00348/JP23K17913). CD measurements were performed with the help of Dr. Takashi Kajitani (Institute of Science Tokyo). Theoretical calculations were performed using computers at the Research Center for Computational Science, Okazaki, Japan (23-IMS-C063, 24-IMS-C060).

## ■ REFERENCES

- (1) (a) Bringmann, G.; Price Mortimer, A. J.; Keller, P. A.; Gresser, M. J.; Garner, J.; Breuning, M. Atroposelective Synthesis of Axially Chiral Biaryl Compounds. *Angew. Chem., Int. Ed.* **2005**, *44*, 5384–5427. (b) Tan, B. *Axially Chiral Compounds: Asymmetric Synthesis and Applications*; Wiley-VCH: Weinheim, Germany, 2021.
- (2) (a) Pu, L. 1,1'-Binaphthyl Dimers, Oligomers, and Polymers: Molecular Recognition, Asymmetric Catalysis, and New Materials. *Chem. Rev.* **1998**, *98*, 2405–2494. (b) Pu, L. Enantioselective Fluorescent Sensors: A Tale of BINOL. *Acc. Chem. Res.* **2012**, *45*, 150–163. (c) Tanaka, H.; Inoue, Y.; Mori, T. Circularly Polarized Luminescence and Circular Dichroisms in Small Organic Molecules: Correlation between Excitation and Emission Dissymmetry Factors. *ChemPhotoChem.* **2018**, *2*, 386–402. (d) Nitti, A.; Pasini, D. Aggregation-Induced Circularly Polarized Luminescence: Chiral Organic Materials for Emerging Optical Technologies. *Adv. Mater.* **2020**, *32*, 1908021.
- (3) Representative examples: (a) Beer, G.; Niederal, C.; Grimme, S.; Daub, J. Redox Switches with Chiroptical Signal Expression Based on Binaphthyl Boron Dipyrromethene Conjugates. *Angew. Chem., Int. Ed.* **2000**, *39*, 3252–3255. (b) Kaufmann, C.; Bialas, D.; Stolte, M.; Würthner, F. Discrete  $\pi$ -Stacks of Perylene. Bisimide Dyes within Folda-Dimers: Insight into Long- and Short-Range Exciton Coupling. *J. Am. Chem. Soc.* **2018**, *140*, 9986–9995. (c) Sato, K.; Hasegawa, M.; Nojima, M. Y.; Hara, M.; Nishiuchi, T.; Imai, Y.; Mazaki, Y. Circularly Polarized Luminescence of a Stereogenic Curved Paraphenylene Anchoring a Chiral Binaphthyl in Solution and Solid State. *Chem.—Eur. J.* **2021**, *27*, 1323–1329.
- (4) (a) Palmans, A. R. A.; Meijer, E. W. Amplification of Chirality in Dynamic Supramolecular Aggregates. *Angew. Chem., Int. Ed.* **2007**, *46*, 8948–8968. (b) Caricato, M.; Sharma, A. K.; Coluccini, C.; Pasini, D. Nanostructuring with Chirality: Binaphthyl-based Synthons for the Production of Functional Oriented Nanomaterials. *Nanoscale* **2014**, *6*, 7165–7174. (c) Yashima, E.; Ousaka, N.; Taura, D.; Shimomura, K.; Ikai, T.; Maeda, K. Supramolecular Helical Systems: Helical Assemblies of Small Molecules, Foldamers, and Polymers with Chiral Amplification and Their Functions. *Chem. Rev.* **2016**, *116*, 13752–13990.
- (5) (a) Chen, L.-J.; Yang, H.-B.; Shionoya, M. Chiral Metallosupramolecular Architectures. *Chem. Soc. Rev.* **2017**, *46*, 2555–2576. (b) Zhao, J.; Zeng, K.; Jin, T.; Dou, W.-T.; Yang, H.-B.; Xu, L. Circularly Polarized Luminescence in Macrocycles and Cage: Design, Preparation, and Application. *Coord. Chem. Rev.* **2024**, *502*, 215598.

(6) Exceptional examples: (a) Tang, X.; Jiang, H.; Si, Y.; Rampal, N.; Gong, W.; Cheng, C.; Kang, X.; Fairen-Jimenez, D.; Cui, Y.; Liu, Y. Endohedral Functionalization of Chiral Metalorganic Cages for Encapsulating Achiral Dyes to Induce Circularly Polarized Luminescence. *Chem.* **2021**, *7*, 2771–2786. (b) Hashimoto, Y.; Tanaka, Y.; Suzuki, D.; Imai, Y.; Yoshizawa, M. Chiroptically Active Host-Guest Composites Using a Terpene-Based Micellar Capsule. *J. Am. Chem. Soc.* **2024**, *146*, 23669–23673. (c) Sasafuchi, H.; Ueda, M.; Kishida, N.; Sawada, T.; Suzuki, S.; Imai, Y.; Yoshizawa, M. Remote Optical Chirality Transfer via Helical Polyaromatic Capsules upon Encapsulation. *Chem.* **2025**, *11*, in press.

(7) Representative coencapsulation: (a) Kim, H.-J.; Heo, J.; Jeon, W. S.; Lee, E.; Kim, J.; Sakamoto, S.; Yamaguchi, K.; Kim, K. Selective Inclusion of a Hetero-Guest Pair in a Molecular Host: Formation of Stable Charge-Transfer Complexes in Cucurbit[8]uril. *Angew. Chem., Int. Ed.* **2001**, *40*, 1526–1529. (b) Yoshizawa, M.; Tamura, M.; Fujita, M. AND/OR Bimolecular Recognition. *J. Am. Chem. Soc.* **2004**, *126*, 6846–6847. (c) Ubasart, E.; Borodin, O.; Fuertes-Espinosa, C.; Xu, Y.; García-Simón, C.; Gómez, L.; Juanhuix, J.; Gándara, F.; Imaz, I.; Maspoch, D.; von Delius, M.; Ribas, X. A Three-shell Supramolecular Complex Enables the Symmetry-mismatched Chemo- and Regioselective Bis-Functionalization of  $C_{60}$ . *Nat. Chem.* **2021**, *13*, 420–427.

(8) Representative coencapsulation by hydrogen bonding capsules; (a) Heinz, T.; Rudkevich, D. M.; Rebek, J., Jr Pairwise Selection of Guests in a Cylindrical Molecular Capsule of Nanometre Dimensions. *Nature* **1998**, *394*, 764–766. (b) Scarso, A.; Shivanyuk, A.; Hayashida, O.; Rebek, J., Jr Asymmetric Environments in Encapsulation Complexes. *J. Am. Chem. Soc.* **2003**, *125*, 6239–6243.

(9) (a) Kondo, K.; Suzuki, A.; Akita, M.; Yoshizawa, M. Micelle-like Molecular Capsules with Anthracene Shells as Photoactive Hosts. *Angew. Chem., Int. Ed.* **2013**, *52*, 2308–2312. (b) Yoshizawa, M.; Catti, L. Bent Anthracene Dimers as Versatile Building Blocks for Supramolecular Capsules. *Acc. Chem. Res.* **2019**, *52*, 2392–2404. (c) Yoshizawa, M.; Catti, L. Aromatic Micelles: toward a Third-Generation of Micelles. *Proc. Jpn. Acad., Ser. B* **2023**, *99*, 29–38.

(10) (a) Kondo, K.; Akita, M.; Nakagawa, T.; Matsuo, Y.; Yoshizawa, M. A V-Shaped Polyaromatic Amphiphile: Solubilization of Various Nanocarbons in Water and Enhanced Photostability. *Chem.—Eur. J.* **2015**, *21*, 12741–12746. (b) Kondo, K.; Akita, M.; Yoshizawa, M. Solubility Switching of Metallo-Phthalocyanines and Their Larger Derivatives upon Encapsulation. *Chem.—Eur. J.* **2016**, *22*, 1937–1940. (c) Catti, L.; Narita, H.; Tanaka, Y.; Sakai, H.; Hasobe, T.; Tkachenko, N. V.; Yoshizawa, M. Supramolecular Singlet Fission of Pentacene Dimers within Polyaromatic Capsules. *J. Am. Chem. Soc.* **2021**, *143*, 9361–9367. (d) Hashimoto, Y.; Katagiri, Y.; Tanaka, Y.; Yoshizawa, M. Solution-state Mechanochromic Luminescence of Pt(II)-complexes Displayed within Micellar Aromatic Capsules. *Chem. Sci.* **2023**, *14*, 14211–14216.

(11) Cycloparaphenylenes (CPPs): (a) Darzi, E. R.; Jasti, R. The Dynamic Size-Dependent Properties of [5]-[12]Cycloparaphenylenes. *Chem. Soc. Rev.* **2015**, *44*, 6401–6410. (b) Segawa, Y.; Yagi, A.; Matsui, K.; Itami, K. Design and Synthesis of Carbon Nanotube Segments. *Angew. Chem., Int. Ed.* **2016**, *55*, 5136–5158.

(12) Multisubstituted CPPs: (a) Lu, D.; Zhuang, G.; Jia, H.; Wang, J.; Huang, Q.; Cui, S.; Du, P. A Novel Symmetrically Multifunctionalized Dodecamethoxy-Cycloparaphenylene: Synthesis, Photophysical, and Supramolecular Properties. *Org. Chem. Front.* **2018**, *5*, 1446–1451. (b) Narita, N.; Kurita, Y.; Osakada, K.; Ide, T.; Kawai, H.; Tsuchido, Y. A Dodecamethoxy[6]cycloparaphenylene Consisting Entirely of Hydroquinone Ethers: Unveiling In-plane Aromaticity through a Rotaxane Structure. *Nat. Commun.* **2023**, *14*, 8091.

(13) CPPs as a guest: (a) Hashimoto, S.; Iwamoto, T.; Kurachi, D.; Kayahara, E.; Yamago, S. Shortest Double-Walled Carbon Nanotubes Composed of Cycloparaphenylenes. *ChemPlusChem.* **2017**, *82*, 1015–1020. (b) Matsuki, H.; Okubo, K.; Takaki, Y.; Niihori, Y.; Mitsui, M.; Kayahara, E.; Yamago, S.; Kobayashi, K. Synthesis and Properties of a Cyclohexa-2,7-anthrylene Ethynylene Derivative. *Angew. Chem., Int. Ed.* **2021**, *60*, 998–1003. (c) Endo, M.; Aoyama, S.; Tsuchido, Y.; Catti, L.; Yoshizawa, M. Umbrella-shaped Amphiphiles: Internal

Alkylation of an Aromatic Micelle and Its Impact on Cavity Features. *Angew. Chem., Int. Ed.* **2024**, *63*, No. e202404088, and ref 7c.

(14) CPPs as a host (reviews): (a) Xu, Y.; von Delius, M. The Supramolecular Chemistry of Strained Carbon Nanohoops. *Angew. Chem., Int. Ed.* **2020**, *59*, 559–573. (b) Fan, Y.; He, J.; Guo, S.; Jiang, H. Host-Guest Chemistry in Binary and Ternary Complexes Utilizing  $\pi$ -Conjugated Carbon Nanorings. *ChemPlusChem.* **2024**, *89*, No. e202300536.

(15) See the Supporting Information.

(16) The alkoxy groups are essential for the efficient encapsulation of **1**. Binaphthol (R = OH; Figure 1e) was hardly bound by  $(AA)_n$  even under various conditions.

(17)  $^1H$  NMR spectrum of  $(AA)_n \cdot (1s)_m$  in  $D_2O$  (Figure S7a) showed significantly broadened guest signals, indicating suppressed guest motion through strong host–guest interactions in the cavity. The host–guest composite was stable even under high dilution conditions (i.e., < 0.01 mM based on AA; Figure S11).

(18) The absorption bands of **1s** were red-shifted upon encapsulation by  $(AA)_n$  due to its aggregation in the cavity. The **1s**-based Cotton effects of  $(AA)_n \cdot (1s)_m$  in water are similar to those of solid **1s** (Figure S13).<sup>15</sup>

(19) The CD spectrum of  $(AA)_n \cdot (1r)_m$  prepared from AA and enantiomer **1r**, showed the mirror image of that of  $(AA)_n \cdot (1s)_m$  (Figure S13).<sup>15</sup>

(20) Solvent-dependent aggregation-induced chiroptical properties: Zhang, K.-F.; Saleh, N.; Swierczewski, M.; Rosspeintner, A.; Zinna, F.; Pescitelli, G.; Besnard, C.; Guénee, L.; Bürgi, T.; Lacour, J. Multistate Aggregation-Induced Chiroptical Properties of Enantiopure Disulfide-Mediated Bispyrene Macrocycles. *Angew. Chem., Int. Ed.* **2023**, *62*, No. e202304075.

(21) For the mechanistic study, the inversed and enhanced Cotton effects of **1s** were suggested by the dihedral angle-dependent DFT analysis (Figure S18).<sup>15</sup> The computed CD spectra showed a positive ( $\varphi = 60\text{--}70^\circ$ ) or negative bond ( $\varphi = 80\text{--}100^\circ$ ) at  $\sim 310$  nm.

(22) Torsion angle-dependent positive/negative Cotton effects (<250 nm): Ishikawa, D.; Mori, T.; Yonamine, Y.; Nakanishi, W.; Cheung, D. L.; Hill, J. P.; Ariga, K. Mechanochemical Tuning of the Binaphthyl Conformation at the Air-Water Interface. *Angew. Chem., Int. Ed.* **2015**, *54*, 8988–8991.

(23) To further support the formation of the guest-within-guest structures in  $(AA)_n \cdot (1-3s/r)_m \cdot (CP)_p$  host–guest composites  $(AA)_n \cdot (5s)_m \cdot (CP)_p$  and  $(AA)_n \cdot (2s)_m \cdot (6)_p$ , were prepared using much bulkier (S)-2,2'-dimethoxy-6,6'-diphenyl-1,1'-binaphthyl (**5s**) and acyclic para-hexaphenylene (**6**), respectively, in the same way.<sup>15</sup> Their CD spectra showed no or quite weak band derived from the guest-to-guest chirality transfer within  $(AA)_n$  (Figure S49 and S50).

(24) Emission lifetime of  $(AA)_n \cdot (2s)_m \cdot (CP)_p$  in  $H_2O$  (9.8 ns) is slightly longer than that of CP in  $CHCl_3$  (7.6 ns) under ambient conditions (Figure S25b). The suppressed aggregation of CPs via uptake of **2s** in the micelle is another possible reason. The ternary composite was also stable under dilution conditions (i.e., < 0.01 mM based on AA; Figure S33b).

(25) The emission quantum yield of CP was estimated to be 30–73% in organic solvent: (a) Darzi, E. R.; Sisto, T. J.; Jasti, R. Selective Syntheses of [7]-[12]Cycloparaphenylenes Using Orthogonal Suzuki-Miyaura Cross-Coupling Reactions. *J. Org. Chem.* **2012**, *77*, 6624–6628. (b) Fujitsuka, M.; Cho, D. W.; Iwamoto, T.; Yamago, S.; Majima, T. Size-dependent Fluorescence Properties of [n]-Cycloparaphenylenes ( $n = 8\text{--}13$ ), Hoop-shaped  $\pi$ -Conjugated Molecules. *Phys. Chem. Chem. Phys.* **2012**, *14*, 14585–14588. (c) Segawa, Y.; Fukazawa, A.; Matsuura, S.; Omachi, H.; Yamaguchi, S.; Irlé, S.; Itami, K. Combined Experimental and Theoretical Studies on the Photophysical Properties of Cycloparaphenylenes. *Org. Biomol. Chem.* **2012**, *10*, 5979–5984.

(26) Covalently functionalized CPs with the highest  $g_{abs}$  value ( $\sim 0.02$ ): Xu, Y.; Steudel, F.; Leung, M.-Y.; Xia, B.; von Delius, M.; Yam, V. W.-W. [n]Cycloparaphenylene-Pillar[5]arene Bismacrocycles: Their Circularly Polarized Luminescence and Multiple Guest

Recognition Properties. *Angew. Chem., Int. Ed.* **2023**, *62*, No. e202302978.

(27) An exceptional example using a covalent host and central chiral molecule: Biedermann, F.; Nau, W. M. Noncovalent Chirality Sensing Ensembles for the Detection and Reaction Monitoring of Amino Acids, Peptides, Proteins, and Aromatic Drugs. *Angew. Chem., Int. Ed.* **2014**, *53*, 5694–5699.

(28) (a) Omagari, T.; Suzuki, A.; Akita, M.; Yoshizawa, M. Efficient Catalytic Epoxidation in Water by Axial N-Ligand-Free Mn-Porphyrins within a Micellar Capsule. *J. Am. Chem. Soc.* **2016**, *138*, 499–502. (b) Noto, N.; Hyodo, Y.; Yoshizawa, M.; Koike, T.; Akita, M. Transition Metal-Free Supramolecular Photoredox Catalysis in Water: A Phenoxazine Photocatalyst Encapsulated in V-Shaped Aromatic Amphiphiles. *ACS Catal.* **2020**, *10*, 14283–14289.